

Reports

1986

Assessment of Economic Heavy Minerals of the Virginia Inner Continental Shelf

C. R. Berquist

C. Hobbs

Virginia Institute of Marine Science

Follow this and additional works at: <https://scholarworks.wm.edu/reports>



Part of the [Geology Commons](#)

Recommended Citation

Berquist, C. R., & Hobbs, C. (1986) Assessment of Economic Heavy Minerals of the Virginia Inner Continental Shelf. Virginia Institute of Marine Science, William & Mary. <https://scholarworks.wm.edu/reports/2315>

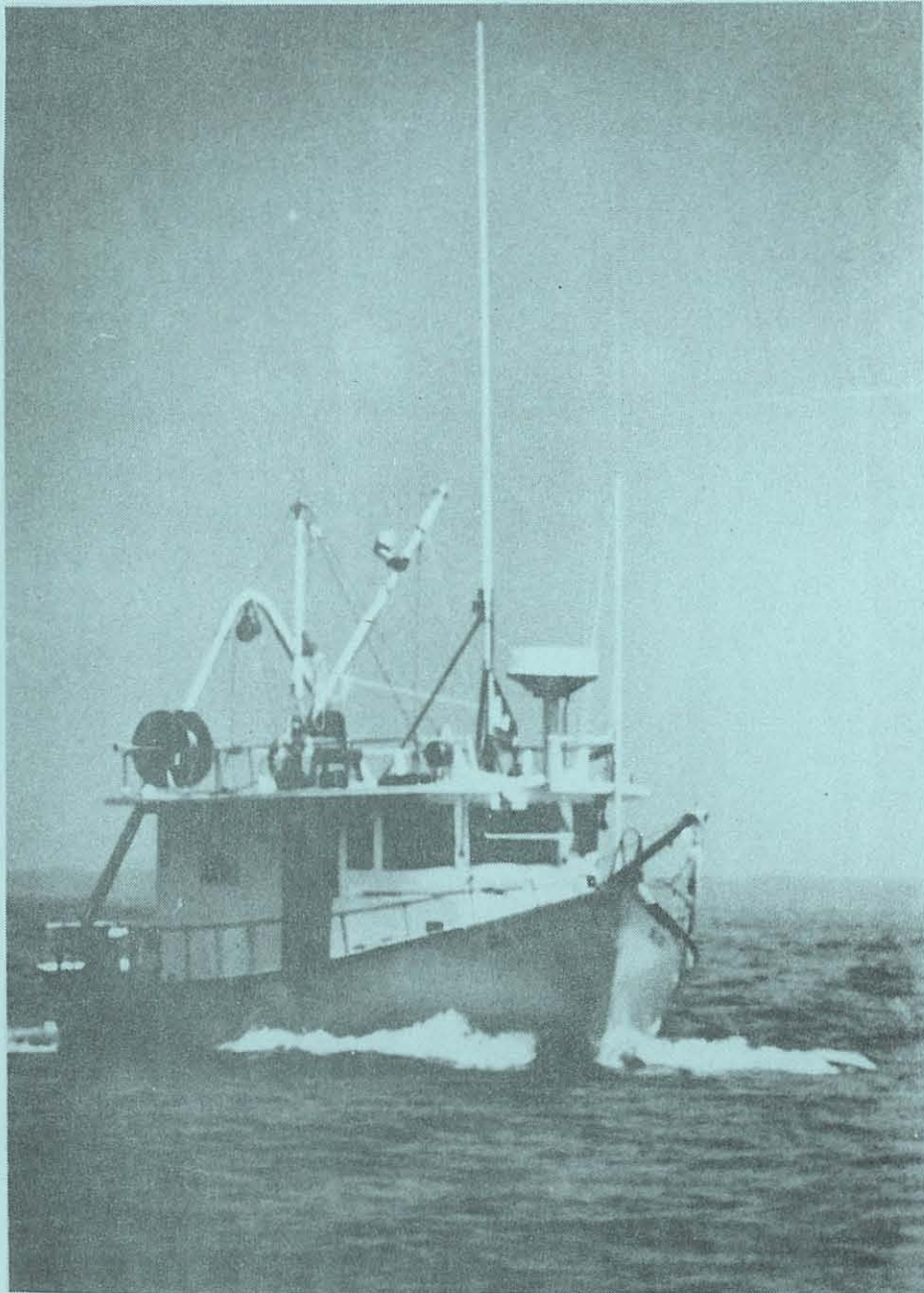
This Report is brought to you for free and open access by W&M ScholarWorks. It has been accepted for inclusion in Reports by an authorized administrator of W&M ScholarWorks. For more information, please contact scholarworks@wm.edu.



VIRGINIA DIVISION OF MINERAL RESOURCES OPEN-FILE REPORT 86-1
VIRGINIA INSTITUTE OF MARINE SCIENCE CONTRIBUTION NO. 1287

ASSESSMENT OF ECONOMIC HEAVY MINERALS OF THE VIRGINIA INNER CONTINENTAL SHELF

C.R. Berquist and C.H. Hobbs



Prepared in cooperation with the
U.S. Minerals Management Service
Contract No. 14-12-0001-30115

FRONT COVER: R/V Langley of the Virginia Institute of Marine Science in route to study area.

Assessment of Economic Heavy Minerals of the
Virginia Inner Continental Shelf

by

C. R. Berquist, Jr.
Virginia Department of Mines, Minerals and Energy
Division of Mineral Resources
Charlottesville, Virginia 22903

C. H. Hobbs, III
Virginia Institute of Marine Science
School of Marine Science
College of William and Mary
Gloucester Point, Virginia 23062

This report was funded in part by the Minerals Management Service, United States Department of the Interior, under a subagreement (Amendment No. 1) Contract No. 14-12-0001-30115 to the Bureau of Economic Geology, The University of Texas at Austin, Austin, Texas.

Contribution No. 1287, Virginia Institute of Marine Science, School of Marine Science, College of William and Mary, Gloucester Point, Virginia.

Copyright 1986, Commonwealth of Virginia

CONTENTS

	Page
Abstract	1
Introduction	1
Acknowledgements	5
Field instrumentation	5
Results	6
Side-scan sonar	6
Subbottom profiler	6
Sample analysis	12
Discussion	12
Smith Island Site	12
Wachapreague and Quinby Inlet sites	12
Conclusions	13
References	13
Appendix A. Location of trackline endpoints	14
Appendix B. Location of samples	15

ILLUSTRATIONS

Figure

1. Regional map	2
2. Detailed location of Smith Island site	3
3. Detailed location of samples W1, W2, and Q1-Q5	4
4. April 1985 cruise; survey grid	7
5. July 1985 cruise; survey lines	8
6. Tracklines for April 1985 cruise	9
7. Interpreted seismic record with sample locations	10
8. Sonar pattern, sample locations, bathymetry	11

TABLE

Analysis of selected samples	16
------------------------------------	----

ABSTRACT

The Virginia Division of Mineral Resources and the Virginia Institute of Marine Science jointly made three cruises over the Virginia continental shelf in April and July of 1985 to sample known heavy-mineral sites for minerals of potential economic and/or strategic value. In addition to sampling, side-scan sonar and sub-bottom profiling surveys were performed at a site off Smith Island. At the Smith Island site, as many as four acoustic horizons were detected within the upper 6 meters of sediment. The uppermost seismostratigraphic layer consists of fine and very fine sand and contains the higher concentrations of heavy minerals. There are also higher concentrations of heavy minerals on the flanks of topographic ridges. The average content of heavy minerals for all samples collected is 8 percent by weight.

INTRODUCTION

In January 1985 the Virginia Division of Mineral Resources entered into a contract with the Bureau of Economic Geology at the University of Texas in Austin (the Bureau acting as "agent" for the Minerals Management Service) to perform a pilot survey that would assess the distribution and concentration of heavy minerals in Virginia's offshore area. This contract was an amendment to a previous subagreement entitled "The Geologic Framework of the Offshore (State and Federal Waters) Adjacent to Virginia with Emphasis on Petroleum Geology" (Contract No. 14-12-0001-30115). The heavy-mineral project was the result of a proposal submitted jointly by the Division of Mineral Resources and the Virginia Institute of Marine Science.

Reconnaissance work by Nichols (1972), Goodwin and Thomas (1973) and Grosz and Escowitz (1983) indicates that extensive sand bodies on the Atlantic Continental Shelf adjacent to Virginia contain heavy minerals of possible economic and/or strategic value. Based on their data, this study was designed to address two main objectives: first, to verify the concentrations of heavy minerals found by the early studies, by locating new samples with greater accuracy; second, to compare heavy-mineral concentrations to bottom morphology, sediment texture, and stratigraphy. Based on the high concentrations of heavy minerals reported in previous work, two sites were selected for surveys and sampling (Figure 1). One site is in a sand-ridge field off Smith Island (Figure 2), the second is in a nearly featureless bottom area off Wachapreague Inlet (Figure 3). The Smith Island site was surveyed with a side-scan sonar to map bottom-surface features and a high-resolution subbottom profiler to identify underlying strata. Because of bad weather, the Wachapreague Inlet area was not surveyed. Both sites and an additional site off Quinby Inlet were sampled however.

This report summarizes the data collected in three cruises. Part of the Smith Island survey site was surveyed and sampled on April 8-11, 1985, using the R/V Langley. High winds and rough seas curtailed this work and prohibited any survey work in the Wachapreague study area. On April 27, 1985, in cooperation with the Maryland Geological Survey, an attempt was made to use a piston corer from their vessel, the R/V Discovery. This attempt was unsuccessful because of hard, well-packed, generally fine-grained bottom sediments. Seven grab samples were taken on the Smith Island site while the R/V Discovery was in the area. On July 22, 1985, additional samples were taken and the Smith Island site was surveyed using

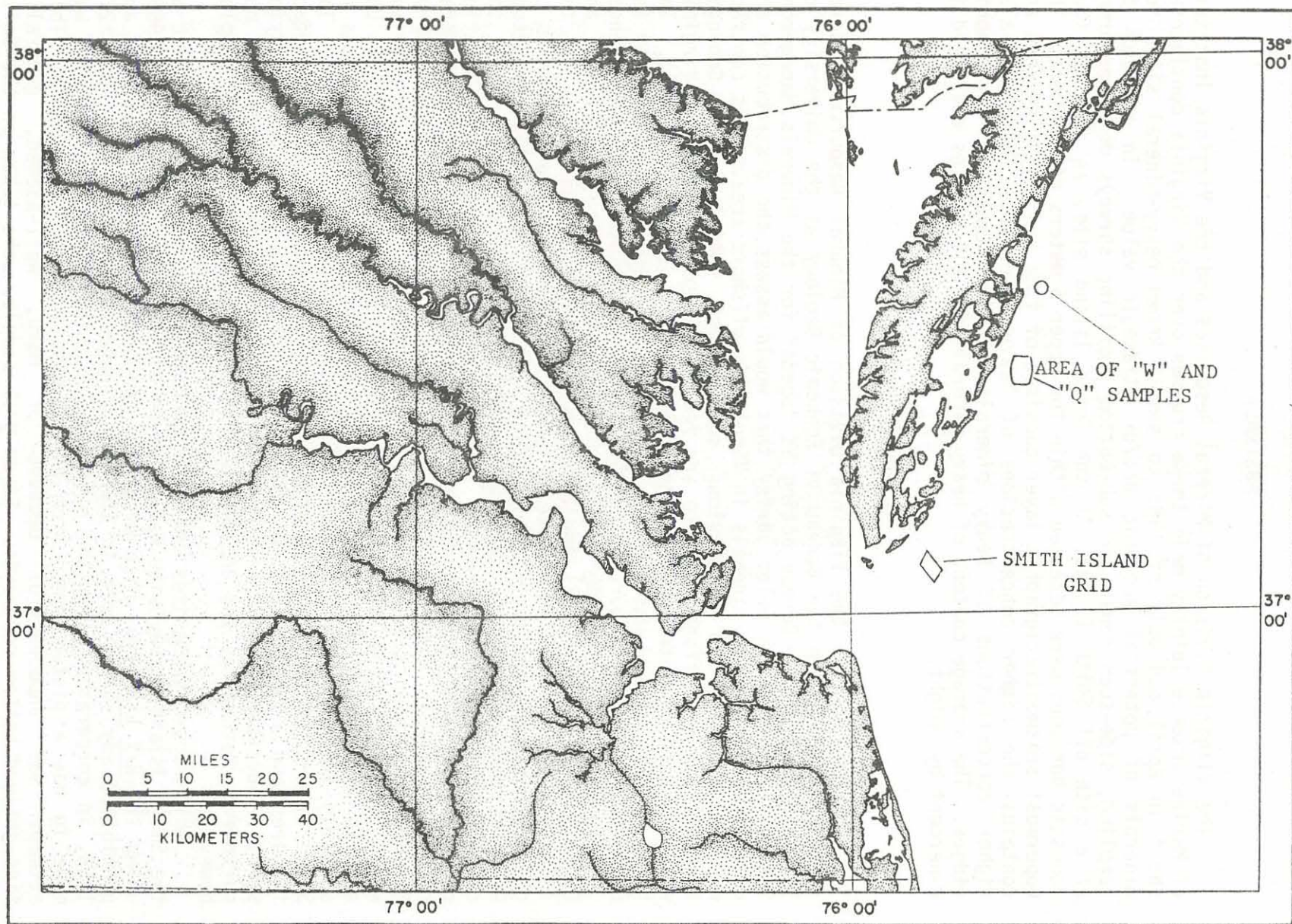


Figure 1. Regional map showing the approximate locations of the final study areas. Circle indicates where "W" samples were taken (marks the proposed northern study area).

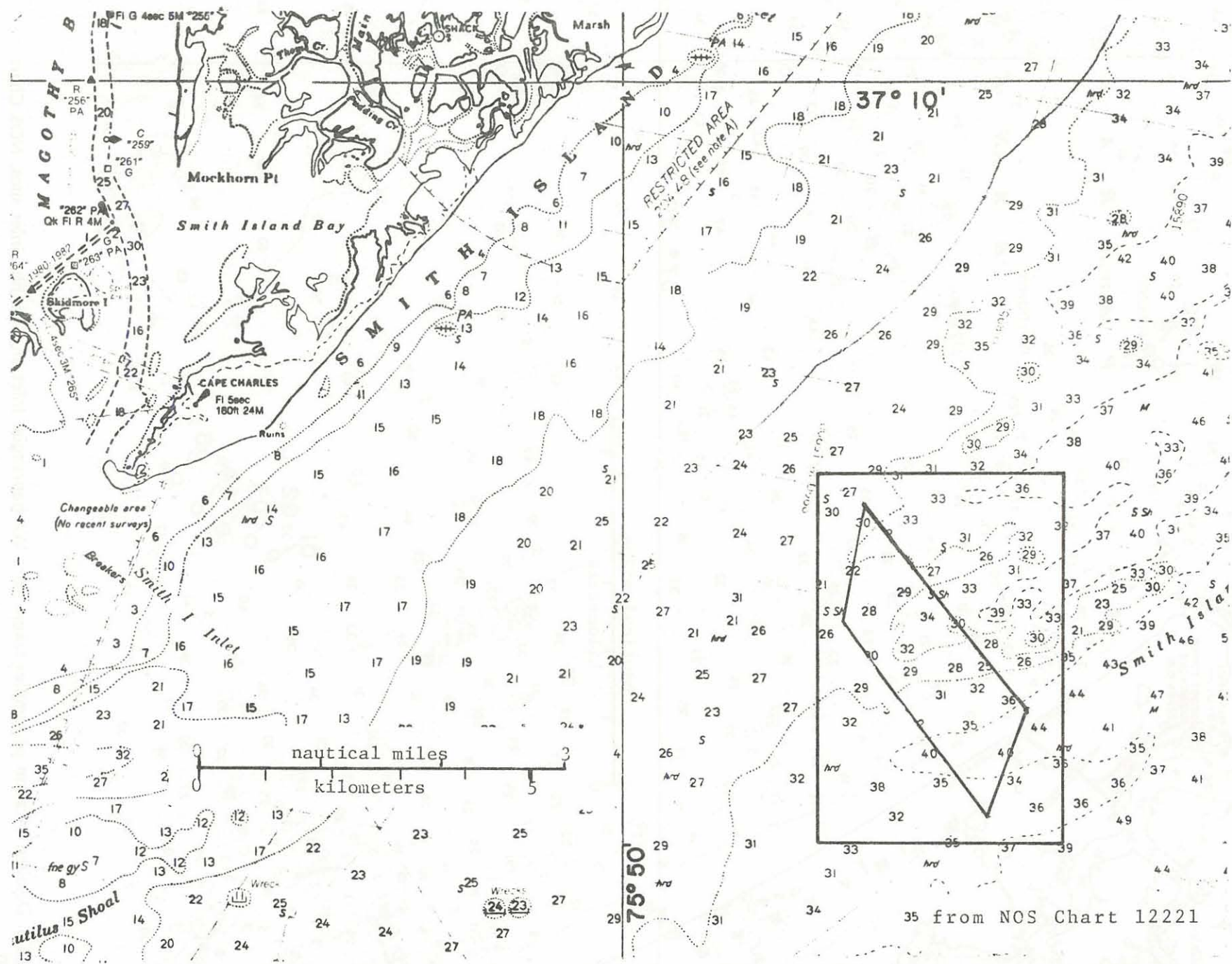


Figure 2. Detailed location of the Smith Island site (grid). Outer rectangle corresponds to computer plot boundaries shown in Figures 4, 5, 6, and 8.

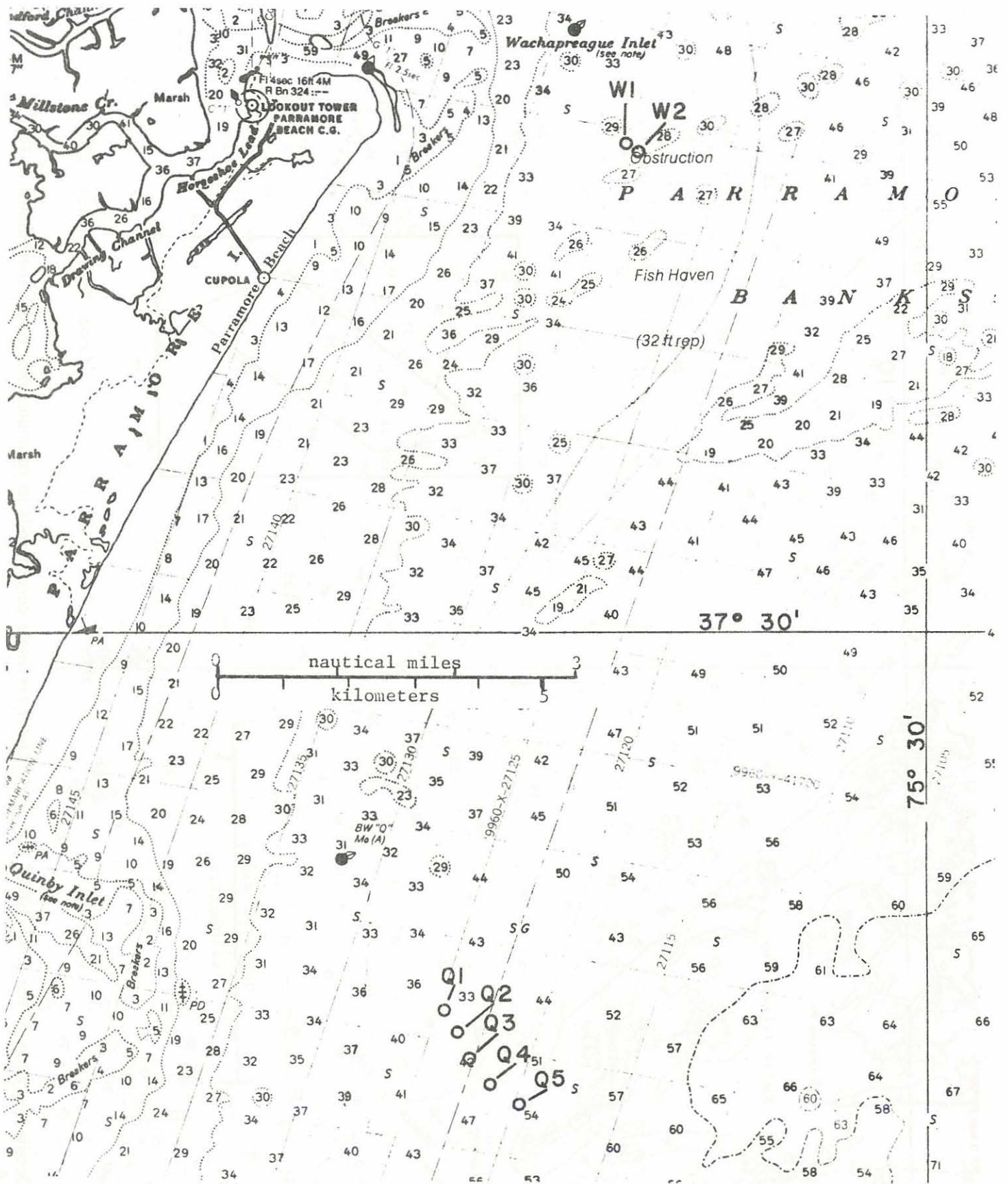


Figure 3. Detailed location of samples taken from Wachapreague Inlet and Quinby Inlet sites, NOS Chart 12210.

the R/V Langley. On July 23 and 24, rough seas again prohibited surveys at the Wachapreague Inlet site however, grab samples were collected from sites at Wachapreague and Quinby inlets.

ACKNOWLEDGEMENTS

We take this opportunity to thank the following individuals whose advice, assistance, and cooperation made the successful completion of this project possible. Mr. S. S. Johnson of the Division of Mineral Resources coordinated the project at the Division, guided our efforts and assisted in the field. Ms. C. C. Mast and Mr. S. A. Skrabal of the Virginia Institute of Marine Science assisted in the field and with the work-up of the data. Mr. J. S. Halka of the Maryland Geological Survey provided the piston and gravity corers and allowed the use of the R/V Discovery while it was in transit between projects. Captains J. Cox, C. Machen, and P. Oliver and Mates S. George and R. Younger of the R/V Langley and R/V Discovery gave invaluable assistance and encouragement.

FIELD INSTRUMENTATION

Three instrument systems, a subbottom profiler, side-scan sonar, and a Ioran microprocessor were used in the acquisition of the field data.

The subbottom profiler is a Datasonics SBP-5000. This system consists of a model SBT-220, two-channel, dual-frequency transceiver, a model TTV-220 towfish to carry the transducers, and the associated tow and electronics cables. The system is used in conjunction with an EPC model 3202 dual channel, graphics recorder. Channel 1, the primary profiling channel, operates on any one of a selectable set of 3.5, 5.0, and 7.0 kHz frequencies or one internally adjustable frequency at a power output that is variable up to a maximum of 12 kw. Channel 2 is fixed at 200 kHz and provides accurate bottom tracking and water depth below the tow vehicle. Channel 2 has a maximum power output of 1 kw. The transceiver has adjustable time variable gain, output pulse duration, and processed signal amplifiers appropriate for a sophisticated acoustic system. The EPC 3202 graphics recorder is a standard, two-channel, graphics recorder that produces a hard copy of the seismic data in real time on special, electrostatic paper. The adjustable sweep rate of the recorder sets both the repetition rate of the transceiver and the scale of the hard copy.

The EG & G model SMS 960 is an advanced side-scan sonar that produces nearly planimetrically correct images of the sea floor. The system uses a model 272 towfish that transmits and receives a 105-kHz, acoustic signal in an arc that is normal to the trackline. During the work for this project, the system was set to scan 100 m (approximately 330 ft) each side of the towfish. The system's chart-paper rate of advance is adjustable and is automatically scaled to the speed of the vessel. When operating in the 100-m half-width, the image is at a scale of 1:10,000. As noted elsewhere in this report, the strength of the reflected signal is indicative of the character of the bottom. Strong reflectors, dark areas on the record, result from hard objects or sediments or from positive relief bottom features, bedforms oriented so as to reflect the acoustic signal directly toward the transducer. Light areas on the record result from poor

reflection, either absorption of the acoustic energy by fine-grained, soft sediments or scattering or shadow zones behind areas of relief.

In order to create mosaics of the side-scan images, to determine the speed of the ship over the bottom (to set the side scan's chart speed), and to be able to return to specific sites, it is necessary to have an accurate and precise navigational system that functions in real time. The R/V Langley is equipped with a Northstar 6500 loran-c receiver-processor. Loran-c is the standard, general-service navigational system for coastal waters. The microprocessor and peripheral additions allow real-time calculations of latitude and longitude (by proprietary software within the microprocessor) and thus, speed over the bottom, heading, and so on. The loran coordinates (time delays) and the other data may be printed automatically on associated equipment.

RESULTS

Side-scan Sonar

Figure 4 indicates the location of survey tracklines acquired during the April cruise aboard the R/V Langley; the darker patterns recorded by the side-scan sonar are also shown. Figure 5 shows tracklines and sonar patterns from the July cruise. The beginning and end of each trackline is numbered and is called a waypoint. The coordinates for the waypoints are listed in Appendix A.

Dark side-scan sonar images result from a strong acoustic reflection off the sea bottom; a light image results from a weak reflection. Bedforms with surfaces facing the transponder and coarse material will give strong reflections; a smooth bottom or soft mud will give poor reflections. Bottom samples collected from dark-pattern areas during the study contain coarser sands than samples collected from the light-pattern areas. Thus, the side-scan patterns appear to be somewhat indicative of bottom texture. Dotted, but unshaded, areas in Figure 4 occur in locations that were not surveyed, but through which adjacent records suggest the continuation of the features.

Comparison of Figures 4 and 5 indicates that the dark side-scan sonar patterns do not exactly coincide. Movement of the bottom sediments during the three months between the surveys may explain the shift. Either the coarse sand moved or the coarse sand was both covered and exposed by moving fine sand. Also the side-scan sonar's transducer was towed from the boat in a different location relative to the loran antenna. This change in tow configuration between cruises coupled with the degree of repeatability of the loran signal and the variations in on-line navigation of the ship may contribute to the pattern shift.

Subbottom profiler

Excellent seismic records were obtained with the high-resolution, subbottom profiler that was towed over the Smith Island grid. Tracklines from this area have been numbered as shown in Figure 6. The best line (line 10) has been interpreted and is shown on Figure 7. Sample locations and areas of dark side-scan sonar patterns are also indicated on Figure 8.

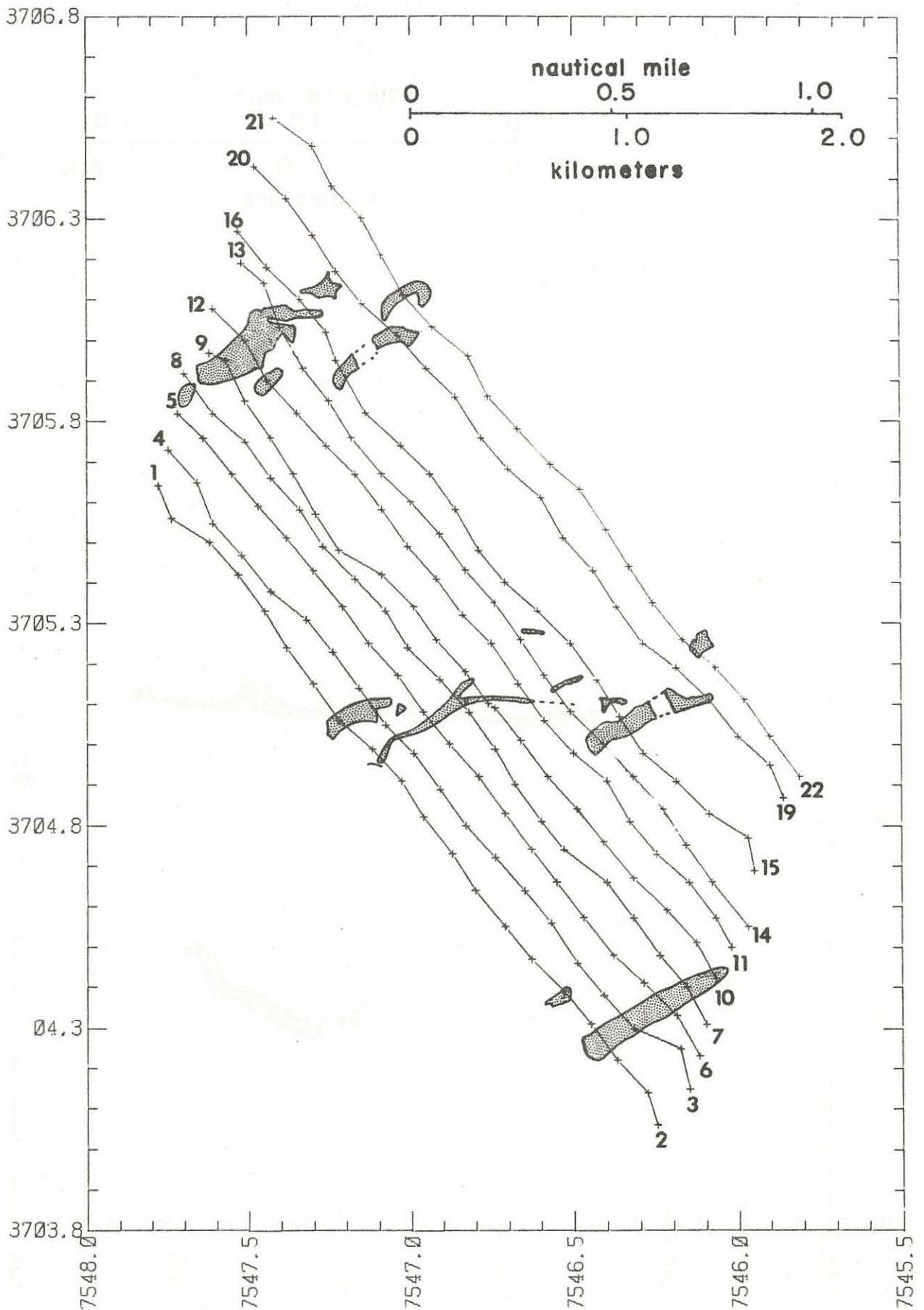


Figure 4. April 1985 cruise; tracklines and dark side-scan sonar patterns. Coordinates are degrees and tenths of minutes of north latitude and west longitude (7545.5 = 75° 45.5'). Waypoints are numbered; their coordinates are given in Appendix A.

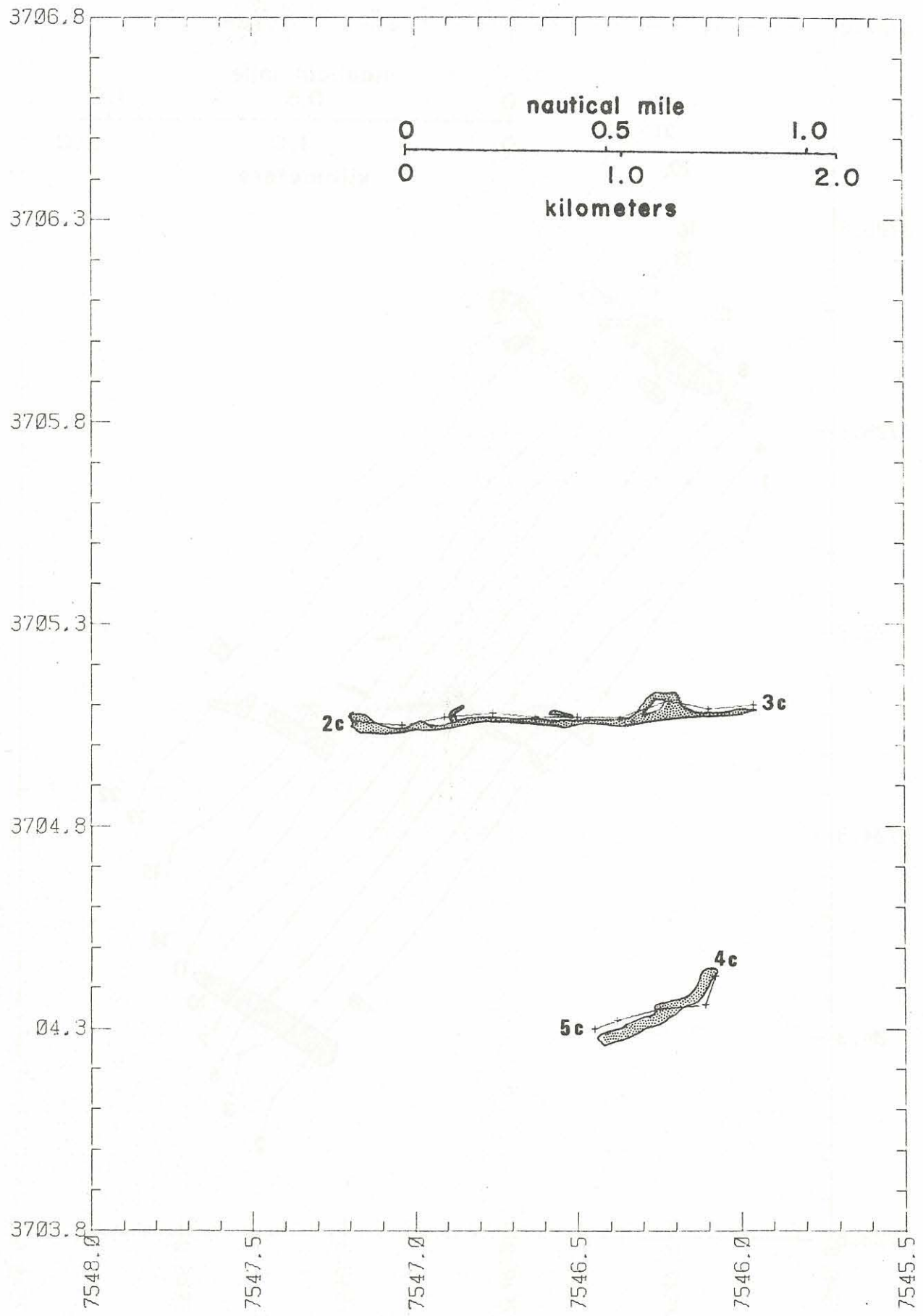


Figure 5. July 1985 cruise; tracklines and dark side-scan sonar patterns. Coordinates are the same as in Figure 4. Waypoint coordinates are given in Appendix A.

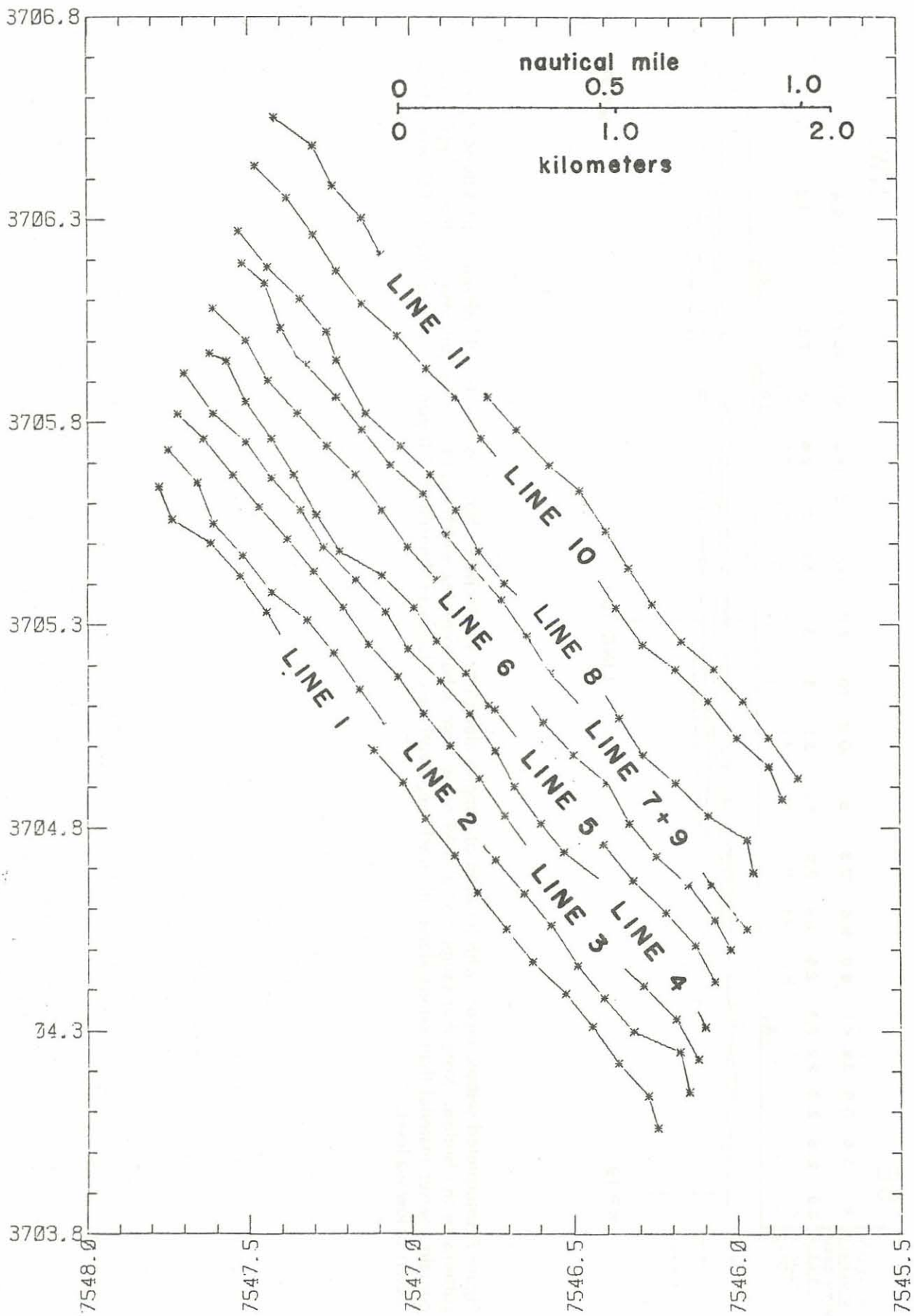


Figure 6. The same tracklines shown on Figure 4 are identified. For clarity, line 9 was removed; it followed approximately the same path as line 7.

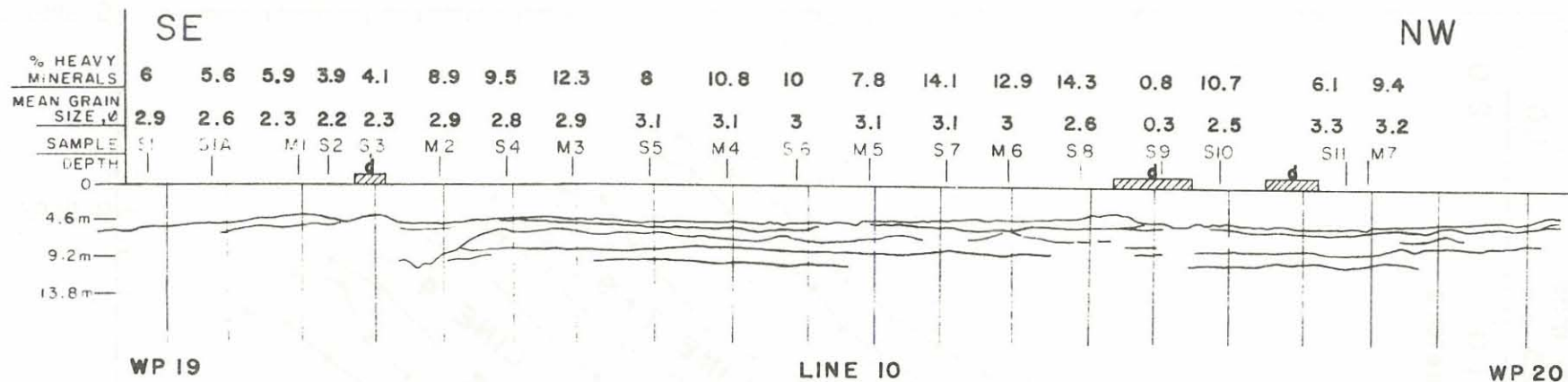


Figure 7. Interpreted seismic record with location of samples along line 10. Hatched boxes marked by "d" identify dark side-scan sonar patterns in the bottom. Note that samples S3 and S9 come from a bottom area which appears to be "uncovered"; these samples also contain coarser material than others along this trackline. Depths are shallower than charted (Figure 2) because the towfish was 4 to 5 meters below sea level.

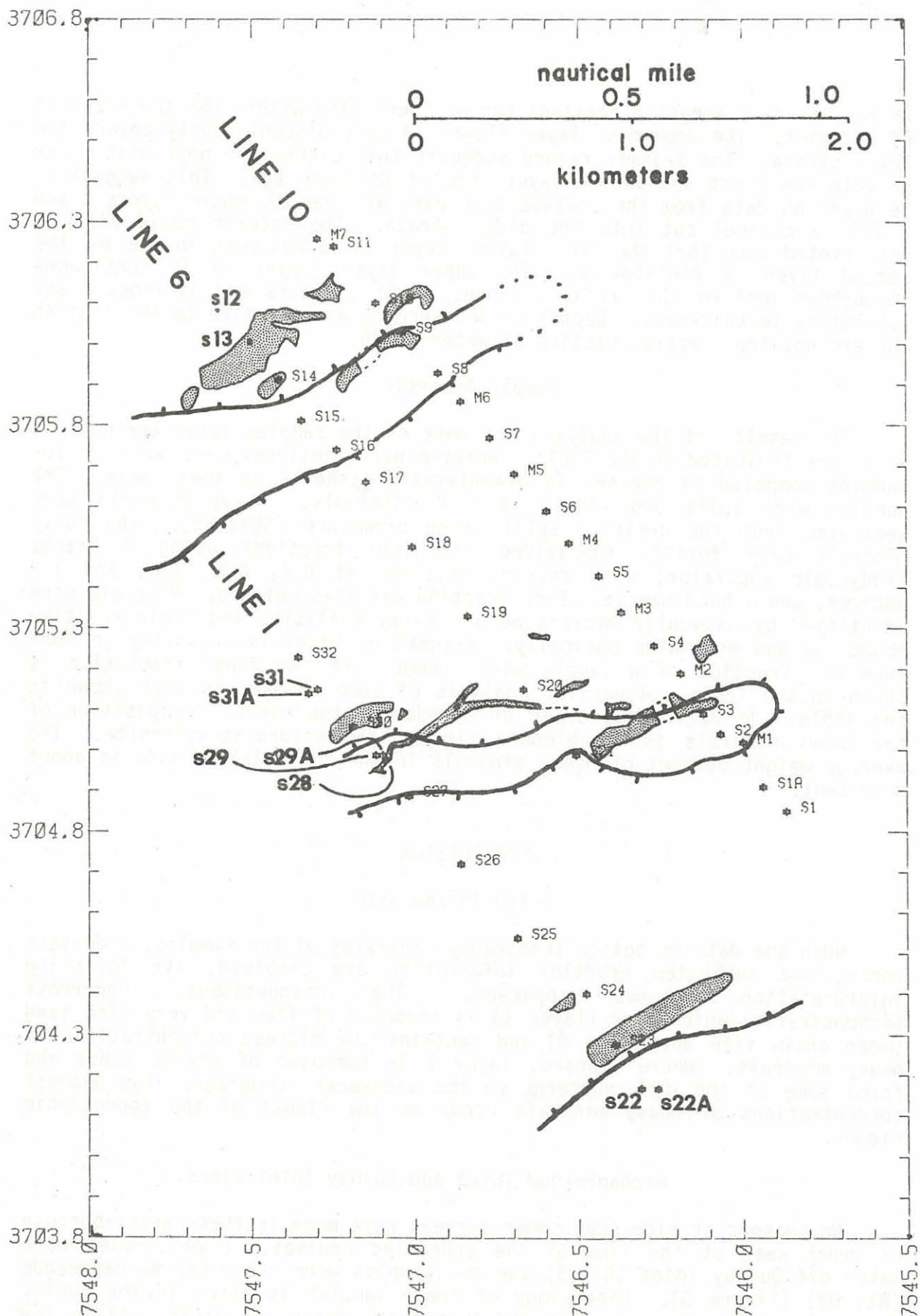


Figure 8. Combined sidescan sonar patterns, sample locations, and relative bathymetry (from subbottom records). Four (4) meter depth contours show tick marks on deeper side of lines. Coordinates of samples are given in Appendix B.

As many as four acoustic horizons can be identified within the top 6 meters of sediment. The uppermost layer (layer 1) only discontinuously covers the lower strata. The seismic record suggests that either the uppermost layer or both the first and second layers are of Holocene age. This suggestion is based on data from the southeastern part of line 10, where layers 1 and 2 fill a channel cut into the older strata. The records could also be interpreted such that the first layer (layer 1) is Holocene in age and the second layer is Pleistocene. The upper layer (layer 1) is continuous throughout most of the profile, ranges up to 3 meters and averages about 1.5 meters in thickness. Depths on the records are relative to the towfish and are not truly representative of water depth.

Sample Analysis

The results of the analyses for most of the samples taken during this study are indicated on the Table. Heavy-mineral analyses were not made for samples composed of coarse- to granular-sized shells or shell hash. The samples were split and sieved at $\frac{1}{2} \phi$ intervals. Heavy minerals were separated from the unsieved split using bromoform (SG=2.85). The heavy minerals were further subdivided into six fractions using a Frantz isodynamic separator, with current settings at 0.4, 0.8, 1.0, and 1.2 amperes, and a hand magnet. Each fraction was then weighed. Minerals were identified by binocular microscope and X-ray analysis, and their relative abundance was estimated optically. Weights of minerals occurring in more than one fraction of a sample were summed, and the final tabulation is shown in the Table. A partial analysis of some samples is also shown in the Table. In decreasing order of abundance, the overall composition of the heavy minerals is hornblende, zircon, and staurolite-ilmenite. The average weight percent of heavy minerals in the Smith Island site is about 8 percent.

DISCUSSION

Smith Island Site

When the data on bottom topography, analyses of the samples, side-scan sonar, and subbottom profiler information are combined, the following interpretation becomes apparent. The discontinuous, uppermost seismostratigraphic layer (layer 1) is composed of fine and very fine sand (mean grain size about 3.0 ϕ) and contains the highest concentrations of heavy minerals. Where exposed, layer 2 is composed of coarse sands and forms some of the dark patterns on the side-scan sonograms. The highest concentrations of heavy minerals occur on the flanks of the topographic ridges.

Wachapreague Inlet and Quinby Inlet Sites

No seismic or side-scan sonar surveys were made in these areas because of rough seas at the time of the scheduled cruises. Five samples were taken off Quinby Inlet (Q1-Q5) and two samples were taken off Wachapreague (W1, W2) (Figure 3). Mineralogy of these samples is shown in the Table. The analyses of these samples indicate that coarse materials contain low percentages of heavy minerals, and that the fine-grained materials contain

high percentages of heavy minerals. These results are similar to the results obtained from the samples collected in the Smith Island site.

CONCLUSIONS

The results obtained from analyses of the samples taken from three sites on the Virginia continental shelf accomplished our first goal, verifying that concentrations of heavy minerals from the bottom surface are high (an average of 8%).

Our second goal was accomplished in the Smith Island area. High concentrations of heavy minerals were found on the surface of a layer of fine sand. This layer is on the flanks of and in the trough between two ridges; it overlies what may be a coarse sand layer with low heavy-mineral concentrations.

Although initial analysis of the results suggests that higher concentration of heavy minerals are confined to a thin, somewhat discontinuous surface layer, this is not necessarily the situation. First, the fine-grained, heavy minerals apparently were concentrated by bottom currents (possibly as a lag?). Layer 1 must have a source. It is quite possible that they are, or were, derived by reworking the underlying strata. Also, because the greater concentrations of the minerals have a specific morphologic setting, the flanks of the topographic highs, and because similar ancient topography may be preserved in the older units, there may be zones of heavy mineral concentrations at depth. A good set of cores, 2 to 10 meters (6 to 30 feet) in length, sampled on the basis of visual differences in stratigraphy, should provide definitive information on the vertical distribution of the placer minerals of interest.

Side-scan sonar and seismic surveys provide an excellent base map for locating areas to sample. A framework has been established that will allow the development of predictive models concerning the origin of these heavy-mineral concentrations. These models may be useful as exploration guides.

REFERENCES

- Goodwin, B. K. and Thomas, J. B., 1973, Inner shelf sediments off Chesapeake Bay III, heavy minerals: Special scientific report number 68, Virginia Institute of Marine Science, 34 p.
- Grosz, A. E. and Escowitz, E. C., 1983, Economic heavy minerals of the U. S. Atlantic continental shelf, in Tanner, W. F. (ed), Proceedings of the sixth symposium on coastal sedimentology: Florida State University, Tallahassee, Florida 32306; p. 231-242.
- Nichols, M. M., 1972, Inner shelf sediments off Chesapeake Bay I, General lithology and composition: Special scientific report number 64, Virginia Institute of Marine Science, 20 p.

APPENDIX A

Location of Trackline Endpoints

Waypoint	Line No.	Latitude ° ' "	Longitude ° ' "	Loran-x	Loran-y
WP1		37 05.64	75 47.78	27141.354	41409.119
WP2	1	37 04.06	75 46.25	27131.942	41393.960
WP3		37 04.15	75 46.15	27131.900	41395.200
WP4	2	37 05.73	75 47.75	27141.515	41410.244
WP5		37 05.82	75 47.72	27141.467	41411.230
WP6	3	37 04.23	75 46.12	27131.913	41396.074
WP7		37 04.31	75 46.10	27131.932	41397.111
WP8	4	37 05.92	75 47.70	27141.608	41412.546
WP9		37 05.97	75 47.62	27141.293	41413.176
WP10	5	37 04.42	75 46.07	27132.021	41398.323
WP11		37 04.50	75 46.02	27131.961	41399.336
WP12	6	37 06.08	75 47.61	27141.492	41414.553
WP13		37 06.19	75 47.52	27141.286	41415.994
WP14	7	37 04.55	75 45.97	27131.802	41400.004
WP15		37 04.69	75 45.95	27132.053	41401.672
WP16	8	37 06.27	75 47.53	27141.513	41416.814
WP19		37 04.87	75 45.86	27131.923	41403.881
WP20	10	37 06.43	75 47.48	27141.638	41418.841
WP21		37 06.53	75 47.43	27141.564	41419.972
WP22	11	37 04.92	75 45.81	27131.857	41404.511
WP2c		37 05.06	75 47.18	27137.816	41403.589
WP3c	Cross 1	37 05.10	75 45.96	27132.700	41406.333
WP4c		37 04.43	75 46.08	27132.081	41398.344
WP5c	Cross 2	37 04.30	75 46.45	27133.413	41396.265

Loran coordinates are for the x and y slaves of the 9960 chain.

Latitudes and longitudes were obtained from automatic conversion of loran coordinates by the loran receiver-processor.

APPENDIX B

Location of Samples

Sample	Latitude	Longitude	Loran-x	Loran-y
S1	37 4.85	75 45.87	27132.001	41403.615
S1A	37 4.91	75 45.94	27132.422	41404.254
S2	37 5.04	75 46.07	27133.162	41405.462
S3	37 5.09	75 46.12	27133.414	41405.865
S4	37 5.26	75 46.27	27134.400	41407.593
S5	37 5.43	75 46.44	27135.365	41409.212
S6	37 5.59	75 46.60	27136.347	41410.744
S7	37 5.77	75 46.77	27137.382	41412.412
S8	37 5.93	75 46.93	27138.361	41413.991
S9	37 6.03	75 47.04	27138.960	41414.934
S10	37 6.10	75 47.12	27139.485	41415.686
S11	37 6.24	75 47.25	27140.204	41416.903
S12	37 6.08	75 47.61	27141.492	41414.553
S15	37 5.81	75 47.35	27139.905	41411.866
S16	37 5.74	75 47.24	27139.337	41411.195
S17	37 5.66	75 47.15	27138.783	41410.593
S19	37 5.33	75 46.84	27136.903	41407.353
S20	37 5.15	75 46.67	27135.856	41405.526
S21	37 4.99	75 46.51	27134.921	41404.130
S22	37 4.17	75 46.31	27132.582	41395.098
S24	37 4.40	75 46.48	27133.769	41397.431
S25	37 4.54	75 46.69	27134.815	41398.573
S26	37 4.72	75 46.86	27135.948	41400.395
S27	37 4.89	75 47.02	27136.819	41401.970
S29	37 4.99	75 47.12	27137.438	41402.940
S31	37 5.15	75 47.30	27138.497	41404.381
S32	37 5.23	75 47.36	27138.872	41405.229
M1	37 5.02	75 46.00	27132.851	41405.370
M2	37 5.19	75 46.19	27133.901	41406.873
M3	37 5.34	75 46.37	27134.977	41408.330
M4	37 5.51	75 46.53	27135.984	41410.038
M5	37 5.68	75 46.70	27136.954	41411.597
M6	37 5.86	75 46.86	27137.933	41413.302
M7	37 6.26	75 47.30	27140.532	41417.175
Q1	37 26.75	75 34.99	27124.9	41672.6
Q2	37 26.58	75 34.83	27123.8	41670.9
Q3	37 26.44	75 34.70	27123.0	41669.5
Q4	37 26.21	75 34.39	27121.2	41667.4
Q5	37 26.02	75 34.15	27119.8	41665.7
W1	37 33.94	75 33.10	27130.0	41757.7
W2	37 33.88	75 32.85	27128.8	41757.4

Loran coordinates are for the x and y slaves of the 9960 chain.

Latitudes and longitudes were obtained from automatic conversion of loran coordinates by the loran receiver-processor.

Table Analyses of selected samples.

Sample number:	S1	S1A	S2	S3	S4	S5	S6	S7	S8	S9	S10	S11	S12	S15	S16	S17	S19	S20	S21	S22	S24	S25
	Weight percent of total sample											Weight percent of total sample										
Heavy minerals	6.0	5.6	3.9	4.1	9.5	8.0	10.0	14.1	14.3	0.8	10.7	6.1	5.5	5.5	16.6	8.7	7.3	6.7	4.4	3.8	6.2	6.8
Gravel	0.22	1.44	0.12	0.23	0.77	0	0.04	0	0.47	13.41	5.89	0.05	0	0.44	0.89	0.64	TR	0	0.13	0.12	0	0.05
Sand	97.80	97.51	99.73	99.57	97.72	97.12	97.38	97.01	98.60	86.45	91.44	94.82	96.08	98.53	98.30	96.95	96.01	97.25	98.76	99.86	95.58	97.75
Mud	1.97	1.04	0.15	0.20	1.51	2.88	2.58	2.99	0.92	0.14	2.67	5.13	3.92	1.04	0.82	2.41	3.99	2.75	1.10	0.03	4.42	2.19
Phi mean grain size	2.89	2.60	2.21	2.26	2.75	3.06	3.04	3.10	2.62	0.31	2.49	3.28	3.19	2.78	2.55	3.06	3.25	3.07	2.76	1.89	3.21	2.99
Phi standard deviation	0.62	0.86	0.59	0.60	0.79	0.62	0.54	0.58	0.77	1.20	1.51	0.59	0.58	0.70	0.89	0.69	0.55	0.59	0.70	0.55	0.61	0.58
	Weight percent of heavy-mineral fraction (S.G. > 2.85)											Weight percent of heavy-mineral fraction (S. G. > 2.85)										
Magnetite (1)	1.9	3.3	TR	TR	3.2	3.7	2.7	3.5	1.6	TR	3.4	3.7			2.0	4.8			4.1	TR	4.0	
Ilmenite	10.6	13.3	8.1	7.5	8.9	12.3	7.6	8.6	7.2	12.8	10.9	8.5			13.0	13.9			12.3	13.7	10.6	
Mica	TR	TR	TR	----	TR	TR	TR	----	TR	TR	TR	TR			TR	TR			TR	----	TR	
Garnet	1.9	2.1	4.9	4.5	1.8	7.0	3.9	1.3	3.6	10.3	1.9	0.6			7.5	0.5			8.2	13.7	14.6	
Epidote	5.7	5.8	7.3	6.0	6.6	2.9	8.9	4.8	4.6	5.1	6.4	11.0			7.7	3.8			5.7	4.8	8.8	
Tourmaline	1.5	2.1	2.4	2.2	1.4	0.4	2.3	1.3	2.0	5.1	1.9	1.2			0.4	1.9			0.8	0.7	0.4	
Hornblende	38.4	29.2	30.9	38.1	26.4	31.3	30.2	26.8	25.2	28.2	22.6	21.3			24.2	42.3			24.6	31.5	39.4	
Staurolite	6.5	8.8	13.0	9.7	5.7	5.8	5.7	9.9	7.4	10.3	11.3	7.3			12.8	11.5			10.7	16.4	5.5	
Rutile	1.5	1.3	0.8	0.7	0.9	0.8	0.9	1.3	0.8	2.6	1.9	1.2			1.6	1.0			1.6	4.1	----	
Sillimanite/kyanite	0.8	0.4	1.6	1.5	0.9	0.8	0.9	----	----	TR	0.4	TR			2.4	3.4			3.3	1.4	2.2	
Pyroxene	11.0	6.7	18.7	9.0	9.8	9.9	10.1	6.7	7.4	5.1	7.2	7.3			2.6	----			0.8	1.4	----	
Sphene	0.8	0.8	TR	0.7	2.3	1.2	0.7	2.2	1.4	5.1	1.1	1.2			2.0	1.0			0.8	1.4	1.5	
Tremolite/actinolite	TR	TR	----	----	----	----	----	----	----	----	----	----			0.4	0.5			0.8	TR	0.4	
Leucoxene	TR	TR	TR	TR	TR	TR	----	TR	TR	TR	TR	TR			----	TR			TR	----	1.1	
Monazite	TR	TR	----	TR	----	----	----	----	----	TR	TR	TR			TR	0.5			1.6	0.7	2.2	
Zircon (2)	18.3	24.6	12.2	17.9	30.5	22.6	23.1	28.8	37.8	10.3	29.4	35.4			15.7	10.1			24.6	10.3	7.3	
Other	0.1	1.6	0.1	2.2	1.6	1.3	3.0	4.8	1.0	5.1	1.6	1.3			7.7	4.8			0.1	----	2.0	
ECON (3)	31.2	39.6	22.7	27.6	41.2	36.5	32.5	38.7	45.8	25.7	42.6	45.1			32.7	28.9			43.4	30.2	23.4	

(1) Magnetite fraction probably includes some magnetic ilmenite.

(2) Zircon fraction may contain some quartz contamination.

(3) ECON defined as sum of percent of ilmenite, rutile, sillimanite, leucoxene, monazite, and zircon.

Table Analyses of selected samples (cont.)

Sample number	S26	S27	S29	S31	S32	M1	M2	M3	M4	M5	M6	M7	W1	W2	Q1	Q2	Q3	Q4	Q5	
	Weight percent of total sample					Weight percent total sample							Weight percent of total sample							
Heavy minerals	5.0	9.2	6.0	9.1	11.6	5.9	8.9	12.3	10.8	7.8	12.9	9.4	2.3	0.6	0.6	3.7	0.6	5.9	3.6	
Gravel	0.03	0.83	0.36	0.82	2.25	0.21	0.25	0.28	0.04	0.14	0.37	0.03	2.36	0.87	28.21	19.52	35.07	2.09	0.44	
Sand	98.76	98.28	98.93	97.07	95.41	99.57	97.48	96.44	96.80	97.71	96.93	95.74	97.14	99.13	70.65	80.40	64.38	96.57	97.81	
Mud	1.22	0.90	0.71	2.11	2.35	0.22	2.27	3.28	3.16	2.15	2.70	4.23	0.50	0	1.14	0.07	0.54	1.33	1.75	
Phi mean grain size	2.84	2.62	2.29	2.82	2.72	2.27	2.97	2.91	3.11	3.07	3.04	3.20	1.69	1.84	0.17	0.76	0.26	2.66	2.88	
Phi standard deviation	0.58	0.76	0.91	0.93	1.11	0.63	0.64	0.79	0.57	0.55	0.64	0.64	0.82	0.64	1.66	1.57	1.66	1.06	0.84	
	Weight percent of heavy-mineral fraction (S.G. > 2.85)										Weight percent of heavy-mineral fraction (S.G. > 2.85)									
Magnetite (1)	4.2		3.3		1.2	3.1	3.9	2.8	2.8	4.5	4.7	2.5						2.0		
Ilmenite	15.4		20.8		13.4	8.7	12.2	9.4	10.6	11.4	13.0	11.4						13.4		
Mica	TR		TR		TR	TR	TR	TR	TR	TR	TR	TR						TR		
Garnet	5.2		6.3		14.3	6.2	6.1	5.7	4.6	6.4	10.6	8.9						2.4		
Epidote	7.0		3.3		3.3	4.2	3.0	7.4	9.2	8.1	5.3	1.3						2.8		
Tourmaline	0.5		1.2		0.6	1.9	1.4	1.7	1.1	1.1	1.0	TR						5.6		
Hornblende	31.6		29.5		19.1	27.4	24.7	21.6	24.6	27.4	27.6	39.2						39.0		
Staurolite	10.2		10.7		14.3	6.9	8.3	9.7	7.7	8.1	8.6	22.8						9.6		
Rutile	1.5		0.9		1.0	1.2	1.2	1.1	----	0.8	0.7	3.8						1.2		
Sillimanite/kyanite	3.0		1.2		0.9	1.2	1.2	1.1	1.1	----	1.3	2.5						1.6		
Pyroxene	2.0		2.7		4.0	5.0	3.7	10.2	9.2	10.6	11.6	2.5						0.2		
Sphene	2.0		2.1		1.2	1.0	1.4	1.1	1.8	0.9	2.7	TR						0.8		
Tremolite/actinolite	0.5		TR		----	----	TR	----	TR	0.5	0.3	TR						0.4		
Leucoxene	TR		TR		TR	TR	TR	TR	TR	TR	TR	TR						0.4		
Monazite	0.2		TR		----	----	----	----	----	----	----	----						TR		
Zircon (2)	16.2		17.6		25.5	31.8	31.2	27.3	26.1	18.4	13.0	2.5						18.1		
Other	0.5		0.4		1.2	1.4	1.7	0.9	1.2	1.8	TR	2.6						2.8		
ECON (3)	36.3		40.5		40.8	42.9	45.8	38.9	37.8	30.6	28.0	20.2						34.7		

(1) Magnetite fraction probably includes some magnetic ilmenite.

(2) Zircon fraction may contain some quartz contamination.

(3) ECON defined as sum of percent of ilmenite, rutile, sillimanite, leucoxene, monazite, and zircon.

Table 1

(a) The following table shows the estimated values of the parameters in the model. The values in parentheses are the standard errors of the estimates. The values in brackets are the t-ratios of the estimates. The values in boldface are the estimates of the parameters of the model.

Parameter	Estimate	Standard Error	t-ratio
α_1	0.15	0.02	7.5
α_2	0.25	0.03	8.3
α_3	0.35	0.04	8.7
α_4	0.45	0.05	9.0
α_5	0.55	0.06	9.2
α_6	0.65	0.07	9.3
α_7	0.75	0.08	9.4
α_8	0.85	0.09	9.5
α_9	0.95	0.10	9.5
α_{10}	1.05	0.11	9.5
α_{11}	1.15	0.12	9.6
α_{12}	1.25	0.13	9.6
α_{13}	1.35	0.14	9.7
α_{14}	1.45	0.15	9.7
α_{15}	1.55	0.16	9.7
α_{16}	1.65	0.17	9.8
α_{17}	1.75	0.18	9.8
α_{18}	1.85	0.19	9.8
α_{19}	1.95	0.20	9.8
α_{20}	2.05	0.21	9.8
α_{21}	2.15	0.22	9.9
α_{22}	2.25	0.23	9.9
α_{23}	2.35	0.24	9.9
α_{24}	2.45	0.25	9.9
α_{25}	2.55	0.26	9.9
α_{26}	2.65	0.27	9.9
α_{27}	2.75	0.28	9.9
α_{28}	2.85	0.29	9.9
α_{29}	2.95	0.30	9.9
α_{30}	3.05	0.31	9.9
α_{31}	3.15	0.32	9.9
α_{32}	3.25	0.33	9.9
α_{33}	3.35	0.34	9.9
α_{34}	3.45	0.35	9.9
α_{35}	3.55	0.36	9.9
α_{36}	3.65	0.37	9.9
α_{37}	3.75	0.38	9.9
α_{38}	3.85	0.39	9.9
α_{39}	3.95	0.40	9.9
α_{40}	4.05	0.41	9.9
α_{41}	4.15	0.42	9.9
α_{42}	4.25	0.43	9.9
α_{43}	4.35	0.44	9.9
α_{44}	4.45	0.45	9.9
α_{45}	4.55	0.46	9.9
α_{46}	4.65	0.47	9.9
α_{47}	4.75	0.48	9.9
α_{48}	4.85	0.49	9.9
α_{49}	4.95	0.50	9.9
α_{50}	5.05	0.51	9.9
α_{51}	5.15	0.52	9.9
α_{52}	5.25	0.53	9.9
α_{53}	5.35	0.54	9.9
α_{54}	5.45	0.55	9.9
α_{55}	5.55	0.56	9.9
α_{56}	5.65	0.57	9.9
α_{57}	5.75	0.58	9.9
α_{58}	5.85	0.59	9.9
α_{59}	5.95	0.60	9.9
α_{60}	6.05	0.61	9.9
α_{61}	6.15	0.62	9.9
α_{62}	6.25	0.63	9.9
α_{63}	6.35	0.64	9.9
α_{64}	6.45	0.65	9.9
α_{65}	6.55	0.66	9.9
α_{66}	6.65	0.67	9.9
α_{67}	6.75	0.68	9.9
α_{68}	6.85	0.69	9.9
α_{69}	6.95	0.70	9.9
α_{70}	7.05	0.71	9.9
α_{71}	7.15	0.72	9.9
α_{72}	7.25	0.73	9.9
α_{73}	7.35	0.74	9.9
α_{74}	7.45	0.75	9.9
α_{75}	7.55	0.76	9.9
α_{76}	7.65	0.77	9.9
α_{77}	7.75	0.78	9.9
α_{78}	7.85	0.79	9.9
α_{79}	7.95	0.80	9.9
α_{80}	8.05	0.81	9.9
α_{81}	8.15	0.82	9.9
α_{82}	8.25	0.83	9.9
α_{83}	8.35	0.84	9.9
α_{84}	8.45	0.85	9.9
α_{85}	8.55	0.86	9.9
α_{86}	8.65	0.87	9.9
α_{87}	8.75	0.88	9.9
α_{88}	8.85	0.89	9.9
α_{89}	8.95	0.90	9.9
α_{90}	9.05	0.91	9.9
α_{91}	9.15	0.92	9.9
α_{92}	9.25	0.93	9.9
α_{93}	9.35	0.94	9.9
α_{94}	9.45	0.95	9.9
α_{95}	9.55	0.96	9.9
α_{96}	9.65	0.97	9.9
α_{97}	9.75	0.98	9.9
α_{98}	9.85	0.99	9.9
α_{99}	9.95	1.00	9.9
α_{100}	10.05	1.01	9.9

Notes: The values in parentheses are the standard errors of the estimates. The values in brackets are the t-ratios of the estimates.

Parameter	Estimate	Standard Error	t-ratio
β_1	0.10	0.01	10.0
β_2	0.20	0.02	10.0
β_3	0.30	0.03	10.0
β_4	0.40	0.04	10.0
β_5	0.50	0.05	10.0
β_6	0.60	0.06	10.0
β_7	0.70	0.07	10.0
β_8	0.80	0.08	10.0
β_9	0.90	0.09	10.0
β_{10}	1.00	0.10	10.0
β_{11}	1.10	0.11	10.0
β_{12}	1.20	0.12	10.0
β_{13}	1.30	0.13	10.0
β_{14}	1.40	0.14	10.0
β_{15}	1.50	0.15	10.0
β_{16}	1.60	0.16	10.0
β_{17}	1.70	0.17	10.0
β_{18}	1.80	0.18	10.0
β_{19}	1.90	0.19	10.0
β_{20}	2.00	0.20	10.0
β_{21}	2.10	0.21	10.0
β_{22}	2.20	0.22	10.0
β_{23}	2.30	0.23	10.0
β_{24}	2.40	0.24	10.0
β_{25}	2.50	0.25	10.0
β_{26}	2.60	0.26	10.0
β_{27}	2.70	0.27	10.0
β_{28}	2.80	0.28	10.0
β_{29}	2.90	0.29	10.0
β_{30}	3.00	0.30	10.0
β_{31}	3.10	0.31	10.0
β_{32}	3.20	0.32	10.0
β_{33}	3.30	0.33	10.0
β_{34}	3.40	0.34	10.0
β_{35}	3.50	0.35	10.0
β_{36}	3.60	0.36	10.0
β_{37}	3.70	0.37	10.0
β_{38}	3.80	0.38	10.0
β_{39}	3.90	0.39	10.0
β_{40}	4.00	0.40	10.0
β_{41}	4.10	0.41	10.0
β_{42}	4.20	0.42	10.0
β_{43}	4.30	0.43	10.0
β_{44}	4.40	0.44	10.0
β_{45}	4.50	0.45	10.0
β_{46}	4.60	0.46	10.0
β_{47}	4.70	0.47	10.0
β_{48}	4.80	0.48	10.0
β_{49}	4.90	0.49	10.0
β_{50}	5.00	0.50	10.0
β_{51}	5.10	0.51	10.0
β_{52}	5.20	0.52	10.0
β_{53}	5.30	0.53	10.0
β_{54}	5.40	0.54	10.0
β_{55}	5.50	0.55	10.0
β_{56}	5.60	0.56	10.0
β_{57}	5.70	0.57	10.0
β_{58}	5.80	0.58	10.0
β_{59}	5.90	0.59	10.0
β_{60}	6.00	0.60	10.0
β_{61}	6.10	0.61	10.0
β_{62}	6.20	0.62	10.0
β_{63}	6.30	0.63	10.0
β_{64}	6.40	0.64	10.0
β_{65}	6.50	0.65	10.0
β_{66}	6.60	0.66	10.0
β_{67}	6.70	0.67	10.0
β_{68}	6.80	0.68	10.0
β_{69}	6.90	0.69	10.0
β_{70}	7.00	0.70	10.0
β_{71}	7.10	0.71	10.0
β_{72}	7.20	0.72	10.0
β_{73}	7.30	0.73	10.0
β_{74}	7.40	0.74	10.0
β_{75}	7.50	0.75	10.0
β_{76}	7.60	0.76	10.0
β_{77}	7.70	0.77	10.0
β_{78}	7.80	0.78	10.0
β_{79}	7.90	0.79	10.0
β_{80}	8.00	0.80	10.0
β_{81}	8.10	0.81	10.0
β_{82}	8.20	0.82	10.0
β_{83}	8.30	0.83	10.0
β_{84}	8.40	0.84	10.0
β_{85}	8.50	0.85	10.0
β_{86}	8.60	0.86	10.0
β_{87}	8.70	0.87	10.0
β_{88}	8.80	0.88	10.0
β_{89}	8.90	0.89	10.0
β_{90}	9.00	0.90	10.0
β_{91}	9.10	0.91	10.0
β_{92}	9.20	0.92	10.0
β_{93}	9.30	0.93	10.0
β_{94}	9.40	0.94	10.0
β_{95}	9.50	0.95	10.0
β_{96}	9.60	0.96	10.0
β_{97}	9.70	0.97	10.0
β_{98}	9.80	0.98	10.0
β_{99}	9.90	0.99	10.0
β_{100}	10.00	1.00	10.0

Notes: The values in parentheses are the standard errors of the estimates. The values in brackets are the t-ratios of the estimates.

Table 2: Summary of the results of the model.

